Scar formation following excisional and burn injuries in a red Duroc pig model

Britani N. Blackstone, PhD[1]; Jayne Y. Kim, PhD[2]; Kevin L. McFarland, MS[3]; Chandan K. Sen, PhD[4]; Dorothy M. Supp, PhD[3,5]; J. Kevin Bailey, MD[6]; Heather M. Powell, PhD[1,2]

1. Department of Materials Science and Engineering, The Ohio State University, Columbus, Ohio,
2. Department of Biomedical Engineering, The Ohio State University, Columbus, Ohio,
3. Research Department, Shriners Hospitals for Children, Cincinnati, Ohio,
4. Department of Surgery and Comprehensive Wound Center, The Ohio State University Wexner Medical Center, Columbus, Ohio,
5. Department of Surgery, University of Cincinnati, Cincinnati, Ohio, and
6. Critical Care, Trauma and Burns, The Ohio State University Wexner Medical Center, Columbus, Ohio

Reprint requests:
Heather M. Powell, The Ohio State University,
116 W. 19th Ave, 243 Fontana Labs,
Columbus, OH 43210
Tel: +6142478673;
Fax: +6142921537;
Email: powell.299@osu.edu

Manuscript received: May 10, 2016
Accepted in final form: June 22, 2017

DOI:10.1111/wrr.12562

ABSTRACT

Scar research is challenging because rodents do not naturally form excessive scars, and burn depth, size, and location cannot be controlled in human longitudinal studies. The female, red Duroc pig model has been shown to form robust scars with biological and anatomical similarities to human hypertrophic scars. To more closely mimic the mode of injury, recreate the complex chemical milieu of the burn wound environment and enhance scar development, an animal model of excessive burn-induced scarring was developed and compared with the more commonly used model, which involves excisional wounds created via dermatome. Standardized, full-thickness thermal wounds were created on the dorsum of female, red Duroc pigs. Wounds for the dermatome model were created using two different total dermatome settings: $\sim$1.5 mm and $\geq$ 1.9 mm. Results from analysis over 150 days showed that burn wounds healed at much slower rate and contracted more significantly than dermatome wounds of both settings. The burn scars were hairless, had mixed pigmentation, and displayed fourfold and twofold greater excess erythema values, respectively, compared with $\sim$1.5 mm and $\geq$ 1.9 mm deep dermatome injuries. Burn scars were less elastic, less pliable, and weaker than scars resulting from excisional injuries. Decorin and versican gene expression levels were elevated in the burn group at day 150 compared with both dermatome groups. In addition, transforming growth factor-beta 1 was significantly up-regulated in the burn group vs. the $\sim$1.5 mm deep dermatome group at all time points, and expression remained significantly elevated vs. both dermatome groups at day 150. Compared with scars from dermatome wounds, the burn scar model described here demonstrates greater similarity to human hypertrophic scar. Thus, this burn scar model may provide an improved platform for studying the pathophysiology of burn-related hypertrophic scarring, investigating current anti-scar therapies, and development of new strategies with greater clinical benefit.

Hypertrophic scars (HTS) are a common form of morbidity resulting from burn injury and surgical procedures, with incidence rates varying from 30 to 91% following burns and 40 to 94% following surgery.[1] HTS develop as a result of a heavily amplified fibroproliferative response during wound healing.[2,3] The underlying pathophysiological mechanisms are incompletely understood. HTS are raised, thick, abnormally pigmented scars that may be firm, pruritic, and painful. In most cases, patients suffering from HTS report a severe impairment of quality of life.[3] Throughout the entire scar maturation period, which can last up to 2 years or more, the scar is actively contracting.[2] Contracture leads to deformity, restriction of mobility, and ultimately, loss of function in the affected areas.[1,2] In addition, HTS exhibit significant erythema, pruritus, pain, burning, and stiffness.[1,2] A large number of therapies, including corticosteroid injections,[4,5] silicone gels,[4,6] pressure garment therapy,[2,7,8] and laser therapy,[4,5,9,10] have been developed in attempts to mitigate the problem of HTS. To date, none of these therapies can completely prevent scarring, and reported outcomes using these therapies vary greatly from highly effective[7,10] to no benefit or even adverse outcomes in some cases.[6,10]

The vast number of treatment options reflects the significant need to treat hypertrophic scarring and the difficulty in conducting tightly controlled scar studies using human clinical trials. As a result, development of a ubiquitously effective treatment option remains elusive.[1,4,5] With unclear efficacies of therapies and unknown mechanisms of action, hypertrophic scar therapy remains challenging

and controversial. Therefore, further HTS research is critical to gain a better understanding of the governing mechanisms and to develop more efficient therapeutic strategies for the prevention and treatment of this devastating condition. Unfortunately, scar studies have a common challenge: the lack of an in vivo model for investigation. Longitudinal studies in the human patient population cannot tightly control for burn depth, size and location, and in most cases, cannot include proper negative controls.[11] To conduct a robust, well-controlled study in a uniform population, an animal model is required.

Many past studies have attempted to use rodents to create valid animal scar models. However, rodent skin does not naturally form HTS and does not have the complex biological and mechanical environment that human skin possesses.[12] A rabbit ear model of hypertrophic scarring was reported after surgeons noticed elevated scar tissue developing after surgical wounding.[13] However, structural parameters observed in human hypertrophic scarring cannot be investigated in this model due to histological differences in rabbit ear skin, including thickness and the healing process over a cartilaginous base.[14] Another rodent scar model was described in tight-skin mice, a mutant mouse strain characterized by firmly attached skin and lack of skin folds.[13] Although the scars developed in this model were characterized by histological similarities as human HTS, these similarities did not persist long-term.[13]

In 1976, a large animal model for excessive scarring was proposed using female red Duroc pigs (FRDPs).[15] In this model, excisional injuries, approximately 6 in. $\times$ 6 in., were created on the dorsal and flank skin of six-week old FRDPs using an air dermatome set to 0.020 in. with three to four passes required to reach a depth where small subcutaneous fat globules were visible. Within four months of the initial injury, a thickened, mixed pigmentation scar with a hyperplastic epithelium and disorganized collagen deposition was observed.[15] More recently, this model has been extensively characterized and shown to exhibit many similarities to human hypertrophic scar, including hypercontraction, hyperpigmentation, disorganized collagen deposition with presence of collagen nodules, and increased numbers of myofibroblasts and mast cells.[11,16–19]

Although this FDRP dermatome model for hypertrophic scarring provides a valuable platform for the study of scar development following surgical excisional injuries, questions remain regarding its utility for modeling scarring after burn injuries. While excisional wounds approximate the physical environment of an excised burn wound, they cannot replicate the biochemical environment of a burn wound. Burn injury induces a cascade of events that differs from excisional injury. Heat causes the excessive generation of reactive oxygen species (ROS), driving lipid peroxidation, and as a result, burn wound progression that continues until ROS are neutralized. Unlike excisional injury, burn injury commonly leads to varying thickness of residual necrotic tissue (clinically extreme presentation as eschar), blistering and increased capillary permeability leading to plasma loss, which persists for up to 48 hours postburn.[20] Additionally, burn injury is associated with a prolonged remodeling phase compared to that of excisional wounds, which may take years to resolve. These differences between excisional wounds and burns may contribute to the disparities observed between human HTS and previously reported FRDP scars. Incorporation of burn injury into a model for HTS merits exploration and may result in a scar that more closely resembles human HTS than excisional wounds.

The goal of this study was to develop and investigate a model for hypertrophic scarring in FRDPs that is inclusive of some of the physiological sequelae of thermal injury. A full-thickness burn model was generated and compared to the dermatome model. Scar morphology and structure were assessed at multiple time points up to 150 days post-injury. Scar biomechanics, erythema, contraction, and gene expression were analyzed in each model.

MATERIALS AND METHODS

Burn injury and animal care

All experiments and data collection were performed following The Ohio State University Institutional Animal Care and Use Committee (IACUC) approved protocols. Four FRDPs (27.5 kg at start of study) were used for the study. Pigs were anesthetized with telazol followed by isoflurane. The dorsal trunk was shaved and sterilized with two alternating 2% chlorohexidine and 70% ethanol scrubs (Butler Schein, Columbus, OH). On each of the four pigs, two burn wounds ($n = 8$ total), one shallow dermatome wound ($n = 4$ total), and one deep dermatome wound ($n = 4$ total) were created on the dorsum. A Zimmer Air Dermatome (Zimmer Inc., Warsaw, IN) with a 5 cm wide plate was used to create tangential excisional wounds (approximately 5 cm $\times$ 5 cm) with a total excised thickness (TET) of $\sim$0.060 in. or $\geq$ 0.750 in. ($N = 4$ per group). Wounds created with a TET setting of $\sim$0.060 in. were considered shallow dermatome (SD) wounds, and wounds created with a TET setting of $\geq$ 0.075 in. were considered deep dermatome (DD) wounds. To confirm the accuracy of the dermatome settings, the excised tissue was measured using a digital dial caliper. Wounds with a TET of setting of 0.060 in. (1.5 mm) ranged from 0.053 to 0.063 in. (mean = 0.062 in.), and wounds with a TET setting of $\geq$ 0.075 in. (1.9 mm) ranged from 0.075 to 0.079 in. (mean, 0.077 in.). Thermal injury was induced using our previously reported custom burn device.[21] The stainless steel stylus (5 cm $\times$ 5 cm) was heated to 200 $\pm$ 10 °C and was pressed to the surface of the skin for 40 seconds at a pressure of three pounds. To examine the initial depth of burn injury, biopsies were collected from select burn wounds immediately after injury. The wounds were photographed immediately after wounding and then covered with nonadhesive Curad gauze pads (Medline Industries, Mundelein, IL) and Tegaderm (3M, St. Paul, MN). Vetrap (3M) bandage tape was wrapped around dorsum and secured with Elastikon (Johnson & Johnson, New Brunswick, NJ). Bandages were removed 7 days post-wounding. A fentanyl patch (NOVAPLUS path, Watson Pharmaceuticals Inc., Parsippany, NJ, 100 mcg) was placed in the pinna of each pig and removed three days postwounding. Qualitative and quantitative assessments described below were performed on all wounds on all pigs for all time points. Pigs were weighed monthly and reported as average weight in kg $\pm$ standard error of the mean (SEM). The

pigs were maintained on standard chow *ad libitum*, fasted overnight before the procedures, housed individually and all were euthanized 150 days postwounding.

Wound closure and transepidermal water loss

The appearance of each wound was inspected at days 10 and 28 postinjury to qualitatively assess healing. Wound reepithelialization and barrier formation were quantitatively assessed at day 28 by measuring transepidermal water loss (TEWL) using a DermaLab Combo unit (Cortex Technology ApS, Hadsund, Denmark). With the probe placed over the center of the wounds, humidity of the air directly above the wound was measured relative to the humidity in the ambient conditions of the environment. Total water loss from the region of the skin was calculated as grams of water lost per square meter of skin per hour, with higher values indicating nonhealed or open wounds.

Scar erythema

At day 150 postwounding, erythema in the scars was quantified relative to that of normal skin. Photographs of each individual scar were taken with an area of normal skin and a color palette in the field of view. Images were normalized in Adobe Photoshop by setting the absolute values for white and black levels using the color palette. Images were converted to the "LAB" color profile using ImageJ (https://imagej.nih.gov/ij/), where "L" is the lightness component, and the chromogenic components are represented by "A" (green to red) and "B" (blue to yellow). The A channel values were separated and used for analysis; exclusively red pixels have the highest "A" value. An area of uninjured skin, including a minimum of 100,000 pixels and excluding hair, was traced and measured on each animal, and mean redness ± standard deviation (SD) were calculated. Scars were traced and the total number of pixels measured; the number of pixels with red values greater than the uninjured skin values was calculated. Scar erythema was calculated as the percentage of scar area with redness greater than that redness mean + SD of normal skin, and is reported as average percent erythema ± SEM.

Scar contraction

Photographs of scars were taken immediately after wounding (day 0) and at 10, 28, 90, and 150 days postwounding. Each scar photograph was taken with a ruler in the field of view for standardization of scar area quantification. Scar contraction was quantified using computer planimetry (Image J[8]) and defined as total scar area (as measured to the outer edge of the hyperpigmented region of scar or the point at which the scar became raise and hairless) at each time point divided by the original scar area (at day 0) × 100. Data are presented as mean percent of original area ± SEM.

Scar morphology and structure

Six mm diameter punch biopsies were taken from each wound at days 10, 28, 90, and 150 days postwounding. All biopsies collected during the study were positioned near but never on the scar edge to reduce any influence of the biopsy on scar maturation. The biopsies were embedded in OCT resin, frozen and stored at −80 °C until sectioning. Sections were stained with hematoxylin and eosin (H&E) to visualize general tissue anatomy. Initial burn injury depth, measured from day 0 biopsies, was quantified as the distance from the top of the tissue to where no individual collagen fibers could be visualized. Total normal skin thickness was measured from control (noninjured) biopsies and measured as the distance from the top of the epidermis to the beginning of adipose tissue. Sections from all groups at days 10, 28, 90, and 150 were immunostained with alpha-smooth muscle actin (α-SMA, Sigma-Aldrich) and von Willebrand Factor (vWF, Sigma-Aldrich) and a nuclear counterstain, 4′,6-diamidino-2-phenylindole (DAPI, ThermoFisher Scientific, Waltham, MA). Slides were imaged using confocal microscopy (FV Filter 1000, Olympus, Waltham, MA) with all image capture settings held constant.

Collagen structure was assessed using picrosirius staining. Sections from days 28, 90, and 150 were stained with Picrosirius Red (Electron Microscopy Sciences, Hatfield, PA) to assess collagen deposition and morphology. Slides were imaged with polarizing light (Axioskop Widefield LM, Zeiss, Oberkochen, Germany) and representative images were reported.

Scar thickness

At day 150 postwounding, scars were excised to fascia and processed for histological sectioning. OCT embedded sections were cut to 10 μm thick and H&E stained. For each scar, two nonoverlapping sections were imaged and scar thickness quantified as the total thickness from the top of the epidermis to the bottom of the dermis. These measurements were made at six locations per section and averaged to represent the total thickness of that scar. Scar thickness for each group was reported as mean ± SEM.

Scar biomechanics

The in vivo biomechanics of normal and scar tissue were evaluated at day 150 using a BTC-2000 (SRLI Technologies, Franklin, TN), which applies negative pressure to the scar and quantifies tissue deformation in response to this load with time. Stiffness, as calculated by the linear region of the pressure–time curve, laxity, the amount of deformation under low load, and elasticity, the amount of instantaneously recovered deformation, were calculated and reported as mean ± SEM. Ex vivo biomechanical properties of each scar were assessed at day 150 by tensile testing to failure. Strips of each scar and of normal skin from each pig (approximately 4 mm × 50 mm) were cut parallel to the dorsal–ventral body axis. The tissue strips were mounted into the grips of a TestResources mechanical tester (TestResources, Shakopee, MN) with the scars positioned centrally within the grips, and strained at 2 mm/second until failure. Elongation at failure, ultimate tensile strength, area under the force-position curve (energy required for breakage), and length of toe-in region were calculated for each sample and reported as mean ± SEM.

Quantitative gene expression analysis

Biopsies collected from the scars at days 10, 28, 90, and 150 were frozen in liquid nitrogen ($n = 4$ per dermatome group, $n = 8$ in burn group). Tissue was ground using a

tissue pulverizer (SPEX SamplePrep, Metuchen, NJ) and total RNA purified using RNeasy Midi Kits (Qiagen Inc., Germantown, MD) according to manufacturer's instructions, except that samples were treated with Proteinase K (Ambion/ThermoFisher Scientific) while in lysis buffer. RNA samples were treated with DNase I (Qiagen, Inc.) prior to synthesis of cDNA using the SuperScript VILO cDNA Synthesis Kit (ThermoFisher Scientific). Quantitative PCR (qPCR) was performed using porcine gene-specific primers for decorin (DCN), versican (VCAN), transforming growth factor-beta 1 (TGF-β1), insulin-like growth factor 1 (IGF1), collagen type I alpha 1 chain (COL1A1), collagen type III alpha 1 chain (COL3A1), matrix metalloproteinase 2 (MMP2), and matrix metalloproteinase 9 (MMP9) (RT^2 qPCR Primer Assays; Qiagen, Inc.), RT^2 SYBR Green qPCR Mastermixes (Qiagen, Inc.) and the iCycler iQ system (Bio-Rad Laboratories, Inc., Hercules, CA). Samples were analyzed using technical triplicates in addition to biological replicates. Expression levels were referenced to the glyceraldehyde 3-phosphate dehydrogenase (GAPDH) gene using the comparative 2-ΔΔCt method[22] to control for mRNA levels per cell. For comparative analyses, expression levels were normalized to the mean expression in all samples at day 10 after injury.

Statistics

Statistical analyses were performed using SigmaPlot (Systat Software, Inc., San Jose, CA) using one way analysis of variance (ANOVA) and multiple pairwise comparisons among groups at each time point, and among different time points for each group, were performed using the Tukey method. Statistical significance was considered at $p < 0.05$. Data are plotted as mean ± SEM.

RESULTS

Initial injury and wound healing

After initial excision, the total thickness of injury in the SD and DD groups was 1.5 ± 0.11 mm and 1.9 ± 0.06 mm, respectively. The dermis was exposed in the dermatome wounds with hair follicles easily seen in the SD group and to a lesser extent in the DD group (Figure 1). In the DD wound group, small pockets of fatty tissue were visible (Figure 1). Initial burn depth was significantly greater than the SD and DD groups at 2.2 ± 0.10 mm deep ($p < 0.01$). Evidence of thermal propagation can be observed outside of the boundaries of the burn stylus (sharp square boundary) immediately after burning (Figure 1). At 10 days post injury, wounds in the SD group appeared to be largely re-epithelialized with only small portions of the central wound visibly open (Figure 1). In contrast, wounds in the DD group remained largely open and moist (Figure 1). All burn wounds appeared larger at day 10 than at day 0 with the burn eschar still intact (Figure 1). By 28 days post injury, the excisional wound groups appeared mostly or completely closed, while the burn group appeared open or covered with scabs (Figure 1). TEWL was not significantly different between normal pig skin and the SD group while both the DD and burn group exhibited significantly greater water loss than normal skin (Figure 2A). TEWL in the burn group was, on average, twofold greater than the DD group and > sixfold greater than the SD group (Figure 2A). All wounds were visibly closed by 40 days (data not shown).

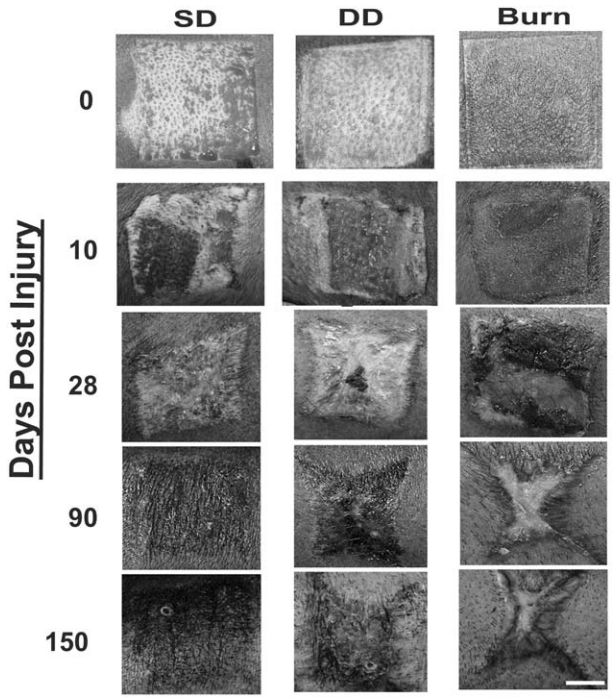

Figure 1. Photographs of injuries at days 0–150 postinjury. A dermatome was used to create excisional wounds with total excised thickness of approximately 0.60 in. (shallow dermatome, SD) or 0.075 in. (deep dermatome, DD). A custom burn device was utilized to create full-thickness burn wounds (burn). By day 28, dermatome wounds have closed whereas the burn injury remains open. At day 150, the burn wounds exhibited substantial contraction with a decreasing amount of contraction observed in the SD and DD groups. Scale bar = 2 cm.

Macroscopic appearance and scar size

During the initial stages of reepithelialization and healing, the scars in all groups were largely hypopigmented with a small rim of hyperpigmentation around the edges of each scar. At days 90 and 150, the central regions of the burn scars remained hypopigmented, whereas scars in the excisional wound groups were hyperpigmented (Figure 1). In addition, at later time points the burn scars were noticeably raised in comparison to the surrounding tissue, while scars in the excisional wound groups were flush with the surrounding tissue (Figure 1). Quantification of scar erythema at day 150 showed a significant increase in scar redness in the burn group compared to both excision groups (Figure 2B).

Following initial injury, all groups increased in size at day 10, followed by contraction to less than their original size by day 28 (Figures 1 and 3). The SD group scars showed little change in shape with time. In contrast, the DD group became more stellate in shape with time and showed signs of contraction at the midpoints of each edge

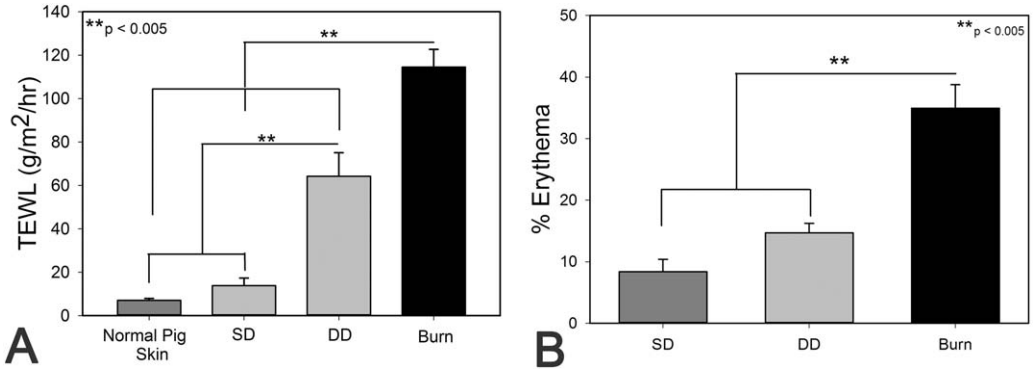

Figure 2. (A) Transepidermal water loss (TEWL) measured at day 28 in all groups and normal pig skin. (B) Percent erythema in dermatome and burn scars after healing for 150 days.

(Figure 1). The burn scars also became stellate in shape with a distinct change in aspect ratio, becoming elongated parallel to the circumference of the pig (Figure 1). Quantitative analysis revealed no significant differences in scar contraction among groups from days 10 to 28. However, by day 90, the burn group showed significantly greater contraction compared with both excisional wound groups (Figure 3). This difference was also seen at day 150 (Figure 3). It is important to note that during this 150 day period, average pig weight increased from 27.5 ± 0.6 kg to 91.9 ± 1.8 kg.

Microscopic characteristics of scars

Histological evaluation of the tissue 10 days following injury showed a marked difference in both extent of injury and state of healing (Figures 4 and 5). Within the SD group, the wound showed signs of reepithelialization with a thin, yet stratified epithelium present. Reepithelialization was not observed in the DD group or the burn group. Vascularization was assessed by immunolocalization of vWF, a marker for endothelial cells, and α-SMA, which is expressed by pericytes around blood vessels. Revascularization was observed in both the SD and DD group by day 10; however newly formed blood vessels were not observed in the burn group (data not shown). Within the burn group, only denatured protein and subcutaneous fat were observed in day 10 histologic sections (Figure 4). By day 28, a stratified epithelium was present in both excisional wound groups with hair follicles observed in the SD group. A highly cellular granulation tissue layer and a thin epidermis were present in the burn group at day 28 (Figure 4). In addition to positive staining for α-SMA in blood vessels, which was observed in all three groups, diffuse dermal staining without vWF colocalization was observed in the burn group at day 28, suggesting expression in myofibroblasts (Figure 5). At day 90, all groups contained a thick, well-stratified epidermis. Hair follicles were only observed in the SD group. At day 150, all groups were well vascularized with all α-SMA colocalized with vWF (Figure 5).

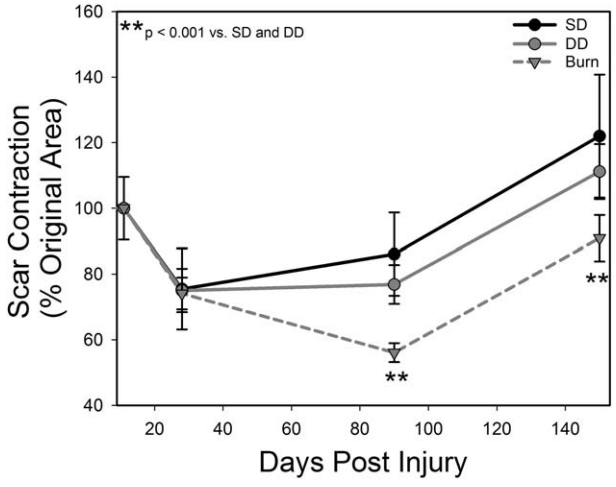

Figure 3. Scar contraction in dermatome and burn scars normalized to initial injury size.

At day 28 postinjury, the dermis of the SD group was comprised of thin, primarily type I collagen with a random organization throughout (Figure 6). The collagen fibers were bundled into thicker reticulations with a more significant fraction of collagen type III fibers (green) in the DD group. A low density of type I collagen fibers (red) oriented perpendicular to the epidermis were visible in the burn group. Collagen density increased in all groups by day 90 with a concomitant rise in the relative abundance of collagen type III staining. Collagen fibers were organized in bundles which increased in thickness from day 28 to day 150 in the DD group and took on an orthogonal ply pattern in this group. Relative abundance of collagen type III decreased in the SD and DD groups at day 150. Collagen density continued to increase in the burn group from day 28 to 150 with a large amount of collagen type III remaining at day 150. Collagen structure was disorganized with many curvilinear bundles of fibers oriented perpendicular to the epidermis. These bundles often surrounded areas with less, dense, more random collagen architecture (Figure 6, white arrow). Additionally, histologic images were used to quantify total scar height, and a statistically significant increase in scar height was observed in the burn group compared to the excision groups (Figure 7).

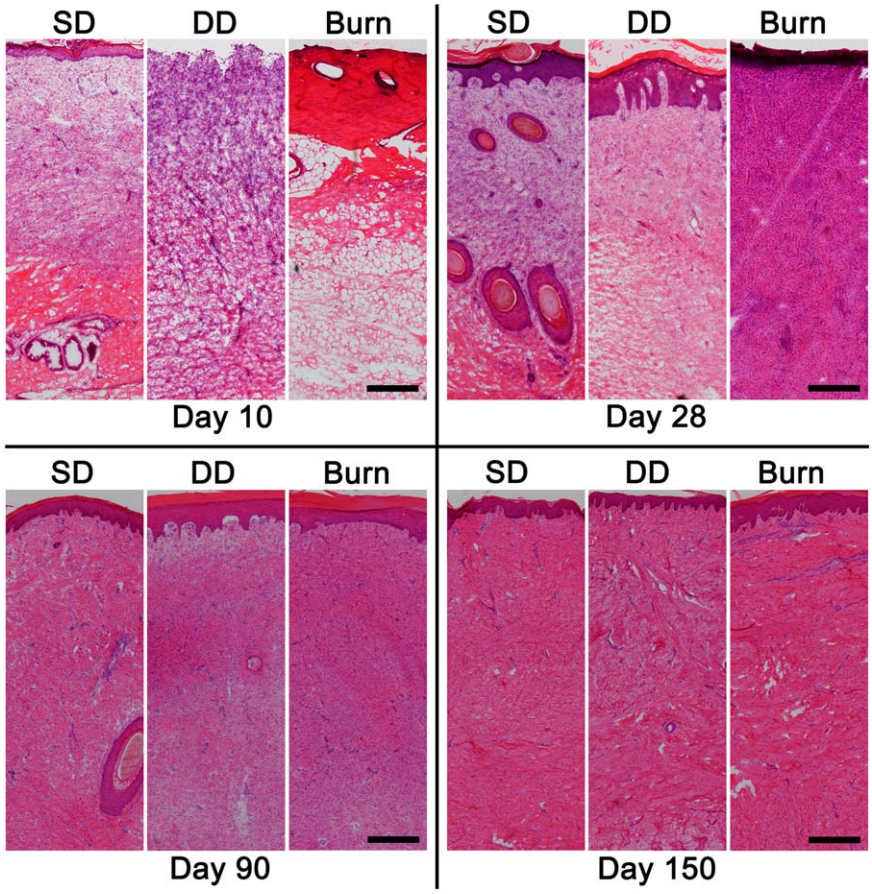

Figure 4. H&E stained histological sections of dermatome (SD, DD) and burn wounds at 10, 28, 90, and 150 days postinjury. Scale bar = 300 μm. [Color figure can be viewed at wileyonlinelibrary.com]

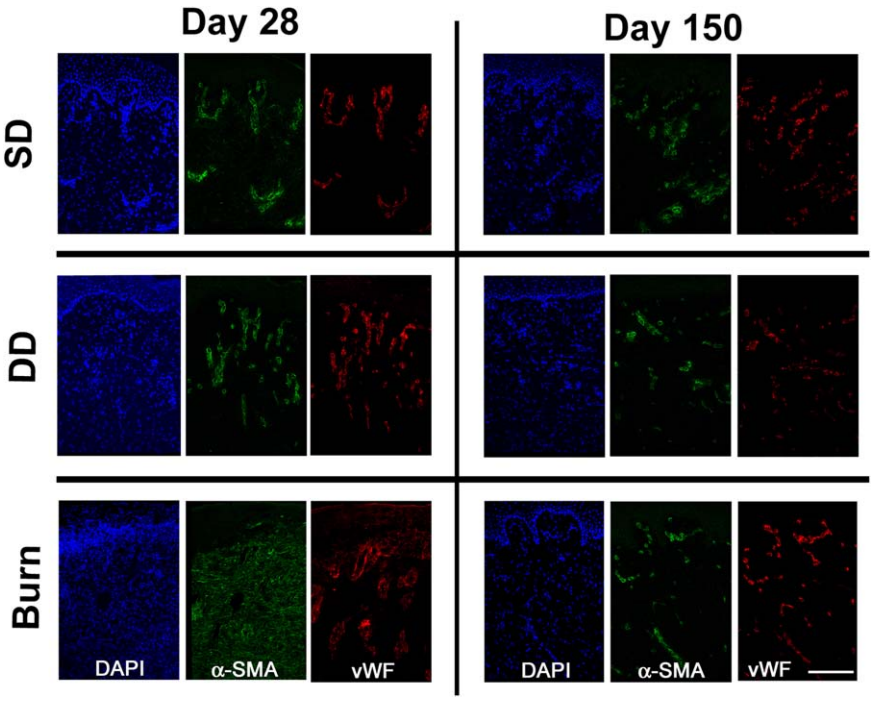

Figure 5. Immunostained cryosections of dermatome (SD, DD) and burn wounds at days 28 and 150 days postinjury. Sections were stained with DAPI and antibodies against α-smooth muscle actin (α-SMA) and von Willebrand factor (vWF). Co-localization of α-SMA and vWF (indicative of blood vessels) was observed for all time points in the SD and DD groups. Myofibroblasts, identified by positive staining for α-SMA only, were observed in the dermis of the burn group at day 28. Scale bar = 150 μm. [Color figure can be viewed at wileyonlinelibrary.com]

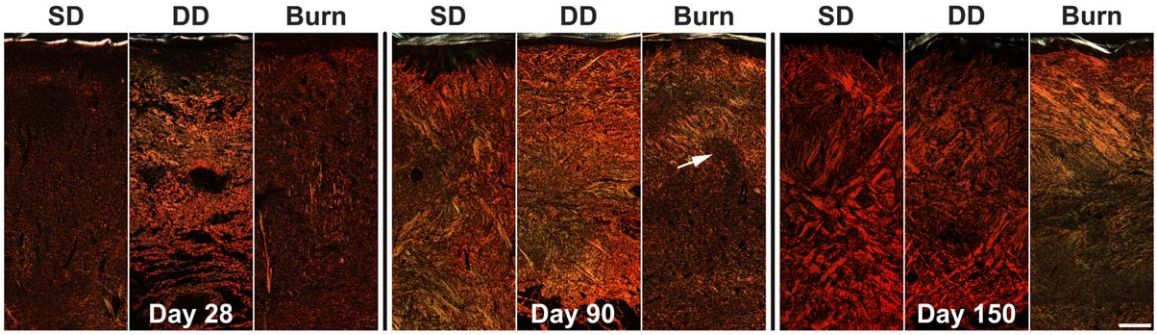

Figure 6. Picrosirius staining sections of porcine scar tissue at days 28, 90, and 150. Collagen type I (red), collagen type III (green). White arrow indicates dense, curvilinear region of collagen surrounding an area of randomly organized less dense collagen, a structure observed in early human hypertrophic scars. Scale bar = 500 μm. [Color figure can be viewed at wileyonlinelibrary.com]

Scar biomechanics

Noninvasive testing of the intact scar tissue showed a moderate increase in stiffness in the burn group compared to control, with a significant amount of variability in tissue stiffness within the SD group (Figure 8A). Deformation of the tissue under low load (i.e., laxity) was significantly reduced in the burn group compared to normal skin (Figure 8B). Elasticity was significantly reduced in the SD and burn groups compared to normal pig skin (Figure 8C). Tensile testing of excised scar tissue at day 150 postinjury showed that the ultimate tensile strength of burn scars and DD scars was significantly weaker than normal skin. In addition, tensile strength of the burn scars was significantly lower than scars in the shallow dermatome (SD) group (Figure 8D). Scars resulting from burn injury were markedly less pliable in tension than all other groups (Figure 8E). The area under the force-position curve was substantially less in the DD and burn group than SD or normal pig skin (Figure 8F). No difference in the length of the toe-in region was observed (data not shown).

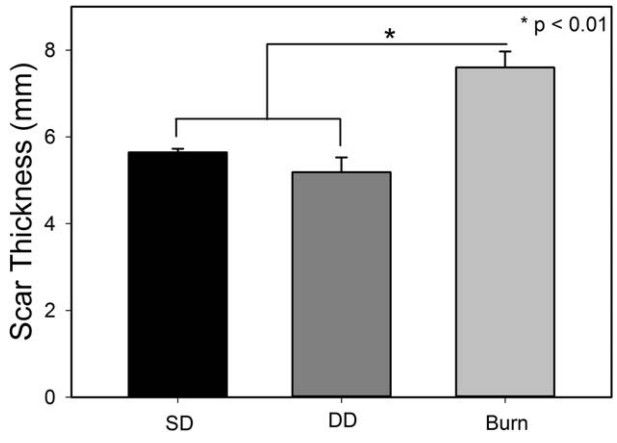

Figure 7. Total scar thickness measured from histological sections at day 150.

Gene expression

Expression of transforming growth factor beta 1 (TGF-β1) showed significant differences among groups at different time points. For all three groups, there was a trend for reduced expression over time; expression at day 150 was significantly lower than all earlier time points in burn scars and was significantly lower than day 10 and day 28 levels in SD and DD scars. Comparisons among groups showed that TGF-β1 expression was significantly greater in burn scars compared to SD scars at all time points, and was also greater than DD scars at day 150 (Figure 9). TGF-β1 expression in DD wounds at day 10 was similar to burn wounds, and was significantly greater than SD wounds (Figure 9).

Analysis of decorin (DCN) expression revealed significant changes over time in all groups (Figure 9). In SD scars, expression increased and was significantly higher at all time points compared with day 10. In DD and burns scars, expression increased over time, with significant increases vs. day 10 in DD scars (days 90 and 150) and burn scars (days 28, 90, and 150). DCN in burn scars at day 150 was significantly higher than at all other time points (Figure 9). Comparisons among groups at each time point revealed significantly greater expression in burn scars compared with SD scars at 150 days after injury (Figure 9).

Versican (VCAN) expression in SD scars and burn scars showed significant differences among different time points; expression peaked at day 28 with significantly elevated expression compared to all other time points (Figure 9). Significant changes with time were not observed for DD scars. VCAN expression in burn scars was greatest at 90 days after injury, with levels at day 90 and 150 significantly higher than at day 10 and day 28. Differences among groups were most evident at later time points. Expression in burn scars was significantly greater than in SD scars at days 90 and 150, and was significantly greater than in DD scars at day 150 (Figure 9).

Expression of insulin-like growth factor 1 (IGF-1) did not change significantly over time in SD wounds (Figure 9). A trend was observed for reduced expression over time for SD and DD scars, but significant differences were only

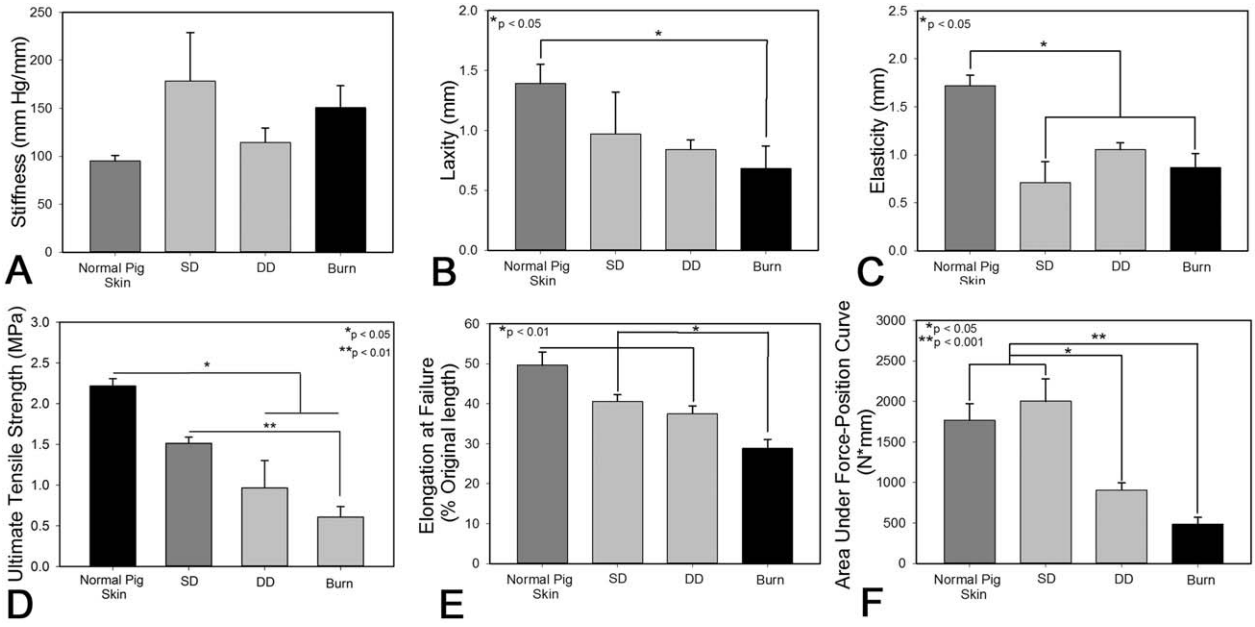

Figure 8. Biomechanical assessment of porcine normal and scar tissue at day 150 postinjury. Noninvasive in vivo measurements of stiffness (A), laxity (B) and elasticity (C) were collected using a BTC-2000. Ex vivo measurements were also collected via tensile testing to failure and quantified ultimate tensile strength (D), percent elongation at failure (E) and the area under the force–position curve (F).

observed between days 10 and 150 in DD scars. In burn scars, IGF-1 expression was highest at day 10 and day 28, with significantly reduced expression at day 90 (vs. day 10 and 28) and day 150 (vs. day 28). Differences among groups at each time point were minimal, with a significant difference observed only between burn and SD scars at day 150 after injury (Figure 9).

Expression of collagen type I alpha chain 1 (COL1A1) and type 3 alpha 1 chain (COL3A1) changed over time, with different patterns observed for dermatome groups compared with the burn group. For both genes, expression in SD and DD scars peaked around the middle of the time course, whereas expression in the burn group peaked near the end of the time course (Figure 9). COL1A1 expression was significantly increased in burn scars at days 90 and 150 compared with day 10, and was significantly greater than in SD or DD scars at days 10 and 28. Expression in DD scars was significantly elevated at day 90 compared with day 10, and was significantly higher than SD scars at this time point. Within the SD and DD groups, peak expression occurred at days 28 and 90 respectively, followed by a slow reduction in expression to baseline. For COL3A1, expression was lowest in burn wounds at day 10, with significantly increased expression at all later time points (Figure 9). Significant increases in COL3A1 expression were observed by day 28 in the SD and DD groups followed a return to baseline values by day 90 (SD group) or day 150 (DD group) (Figure 9). Significant differences among groups were observed between burn and SD scars at days 10 and 150, and between DD and SD scars at day 90.

Expression of MMP2 peaked at day 28 for all three groups (Figure 9). For SD scars, expression at days 90 and 150 was significantly reduced compared with day 10. For burn scars, expression at days 28 and 90 was significantly increased compared with day 10, and although expression at day 150 was significantly reduced (vs. day 28), levels were still elevated compared with day 10. Expression of MMP2 in DD scars did not significantly change with time after injury. The greatest differences among groups were observed between SD and burn scars, with significant differences observed at days 90 and 150. In contrast with MMP2, expression of MMP9 showed the greatest increases at 10 and 28 days after injury, with levels in all three groups at or below day 10 levels at days 90 and 150 (Figure 9). At day 10, MMP9 expression in DD scars was significantly elevated compared to all other time points, and compared with SD and burn scars at day 10. MMP9 expression in burn scars peaked at day 28, with levels significantly increased compared to both other groups and burn scars at all other time points. Relatively low expression was seen in all three groups at 90 and 150 days post injury. No significant change in MMP9 expression with time was detected in the SD group.

DISCUSSION

The reestablishment of epidermal-dermal communication via reepithelialization is critical to the normal wound healing process as this cross-talk modulates the release of many soluble factors that affect cell behavior and ECM production. Delays in this process have been linked to the development of fibrosis[23–25] and it has been previously reported that, in humans, HTS is more prevalent in wounds that require greater than 3 weeks to heal.[23] Zhu et al. reported that deeper dermatome wounds, classified as wounds created with a total excised thickness of 1.5 mm and $\geq$ 1.9 mm,

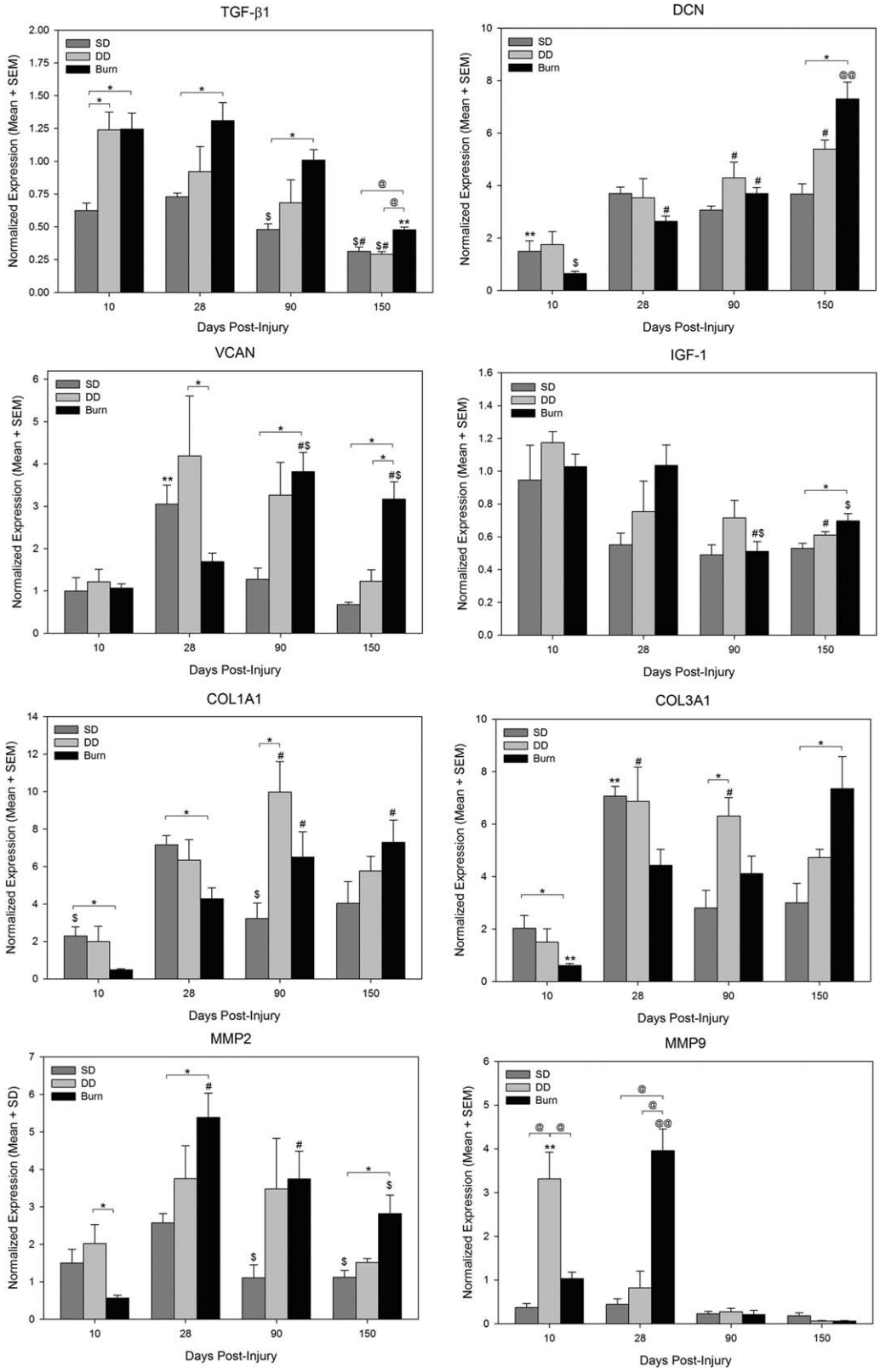
TGF-β1
DCN
VCAN
IGF-1
COL1A1
COL3A1
MMP2
MMP9
SD
DD
Burn
Normalized Expression (Mean + SEM)
Normalized Expression (Mean + SD)
Days Post-Injury
10
28
90
150

Figure 9. Gene expression of transforming factor-beta 1 (TGF-β1), decorin (DCN), versican (VCAN), insulin-like growth factor-1 (IGF-1), collagen type I alpha 1 chain (COL1A1), collagen type III alpha 1 chain (COL3A1), matrix metalloproteinase 2 (MMP2), and matrix metalloproteinase 9 (MMP9) at different times after injury. Dark gray bars represent expression in superficial dermatome (SD) wounds, light gray bars represent expression in deep dermatome (DD) wounds, and black bars represent expression in burn wounds. Expression levels for each gene were normalized to the mean expression in all wounds at day 10. Statistically significant comparisons are indicated by symbols: *, $p < 0.05$ for indicated comparison; @, $p \leq 0.001$ for indicated comparison; #, $p < 0.05$ vs. same group at day 10; $, $p < 0.05$ vs. same group at day 28; **, $p < 0.05$ vs. same group at all other time points; @@, $p \leq 0.001$ vs. same group at all other time points.

were not healed by week 3 postwounding,[12] and wounds 1.14 and 1.5 mm needed 6–8 weeks to reepithelialize.[26] In this current study, all shallow dermatome wounds with a total excised thickness of approximately 1.5 mm were completely healed at day 28 and showed no statistical difference in epidermal barrier function compared to normal pig skin. As adnexa including hair follicles were not removed as part of the excision injury in the SD group, it is not surprising that this group had rapid healing and reestablishment of barrier function as the epidermal cells lining the hair follicles participate in reepithelialization.[27] Barrier function of dermatome wounds with a TET $\geq$ 1.9 mm was significantly decreased from normal pig skin, though the wounds were largely healed visually at 4 weeks postinjury. Burn scars, however, remained open using visual inspection and via TEWL measurements, which were double those of deep dermatome wounds and an order of magnitude greater than normal pig skin. The increased time to heal in the burn wounds was expected as the initial injury is more significant, not only destroying the tissue immediately beneath the burn stylus (with accompanying persistence of nonviable tissue) but also triggering a cascade of events in the surrounding tissue that can lead to damage in the area surrounding the contact region. Previous work with female domestic pigs by Macri et al. utilized a comb burn model where four contact burns were made, separated by 5 $\times$ 20 mm unburned "interspaces," and either left to heal or excised to the wound margins.[28] In both cases, the interspaces were 100% necrotic and/or apoptotic within 7 days of injury.[28] This was contrasted with control wounds having the same dimensions as the comb burner but created by excising unburned skin; in this case, interspaces remained viable[28] and supported improved healing and scarring over burn injuries. As hypertrophic scars are often observed following injuries that are allowed to heal spontaneously,[29] the remaining damaged or necrotic tissue involved in the initial injury may exacerbate scar formation by delaying healing and prolonging inflammation. A prior study comparing wound healing in porcine burn wounds which were debrided immediately following injury or left untreated showed a decrease in the rate of healing and reepithelialization in the nondebrided group though they reported no difference in scarring between these groups at 28 days postinjury.[30]

Human HTS is characterized by abrupt edges, hair loss, hyperpigmentation, erythema, and contraction.[13] SD scars were hyperpigmented, contained hair and had a gradual increase in thickness from the scar edge toward the center. Additionally, these scars contracted very little over the 150 day experiment and displayed little erythema in excess to that of normal skin. When dermatome wounds were generated at greater depths, scar contraction and excess erythema increased slightly and no hair was present within the scars. The scars formed using the burn model were hairless, hypo/hyperpigmented and significantly more contracted than both SD and DD scars. However, like the dermatome scars, none demonstrated abrupt edges; the boundaries between scarring and uninjured skin were more gradual. These findings are in contrast with prior studies reporting on the dermatome model which reported hairless, thick scars in dermatome injuries with total thicknesses of 1.5 mm and $\geq$ 1.9 mm.[12] A possible mechanism for these observed differences is a difference in initial depth. The thickness of the excised tissue was validated in the current study using a digital caliper. It is possible that the depths of the wounds in the prior studies were deeper than the dermatome setting. Full-thickness excisional wounds in red Duroc pigs were observed to contract dramatically with scar area less than 20% of original area just 70 days post injury.[11] While the burn depth measured via histology of tissue immediately following injury was only 16% deeper than the excised thickness of the deep dermatome wounds, the total thickness of tissue involved in the burn injury was likely deeper[28] and may also contribute to the observed increases in contraction and scarring. Cubison et al. reported an HTS incidence of 92% for human wounds that required more than 30 days for healing,[31] suggesting that the slower to heal burn wounds in this study had greater potential to consistently produce scars more similar to human HTS, and another potential parallel of this model of healing.

Additionally, human hypertrophic scars are characterized by their lack of pliability. In ex vivo testing of human HTS and normal skin, HTS was significantly less extensible, requiring significantly more energy to be stretched than normal skin.[32] While all of the scars in these studies were, on average, weaker, less extensible, less elastic, and required more energy to break than normal pig skin, the burn group's biomechanics were substantially inferior to that of normal skin. Interestingly, the stiffness of the scars was not significantly different than normal skin in in vivo and ex vivo testing. Prior studies have observed this phenomenon and hypothesize that alterations in collagen fiber organization, including increases in alignment, cause a reduction in extensibility that is perceived in vivo as greater stiffness.[32]

At a histological level, scars are structurally different than uninjured skin, both in the epidermis as well as the dermis. In the current study, burn scars at day 90 displayed a lack of elongated rete ridges, which is similar to the poor rete ridge regeneration and epidermal flattening that is seen in human HTS.[7,33] This altered state of the HTS epidermis is thought to play a role in the development of

fibrosis in the dermis.[34] Keratinocytes from HTS display increased proliferation[35] and an activated phenotype that is generally found in early stage wound healing.[24] Ghahary et al. reported that, unlike differentiated keratinocytes, proliferating keratinocytes were not able to secrete keratinocyte-derived anti-fibrogenic factor, stratifin, which is known to stimulate fibroblast release of collagenase.[36] In the dermis, all groups exhibited abnormal collagen organization and prominent bundles of collagen. In the SD and DD groups, an orthogonal ply pattern was observed and was reported to be a result of the extracellular matrix responding to stress, likely from contractile forces.[37] Collagen was organized into thinner bundles with linear or curvilinear structure and often clustered around areas with highly random organization. This structure has been previously reported in human HTS during the early stages of development prior to the generation of collagen nodules that are observed as the scar matures.[37] Prior studies using deep excisional wounds observed collagen nodules in the FRDP scars but not until 5 months postinjury and only in a fraction (four of the seven animals studied).[38] It is possible that with additional time collagen nodules may form, however, experimentation would be needed to substantiate this hypothesis. Additionally, the observed pattern of α-SMA staining in these scars, in the absence of vWF colocalization, showed little to no myofibroblasts in the SD and DD groups at all time points, whereas a significant number of myofibroblasts were present in the early phases of burn scar development. In human hypertrophic scars, myofibroblasts are often observed in greater number during early scar development and are reduced in number in more mature scars.[39] While this transition often occurs 2–12 months postinjury,[39,40] the number of fibroblasts in porcine scars appears to peak far sooner, as evidenced by the current data and prior reports using an excisional model.[38] This increase in the rate of scar maturation may also suggest that the porcine scar model is suitable for assessing efficacy of interventions using shorter treatment regimens.

TGF-β is involved in many wound healing processes, including inflammation, fibroblast proliferation, collagen synthesis, and contraction and has been implicated in the development of fibrosis.[41] TGF-β1 mRNA has previously been found to be significantly greater in human HTS [42] and in deep dermatome FRDP wounds[17] than in uninjured skin. Here, TGF-β1 expression peaked 10 days after injury and generally decreased over time, with burn scars expressing significantly more TGF-β1 then SD scars at every time point and more than DD scars at day 150. Decorin has been shown to sequester TGF-β and is a known mediator of proper collagen fibrillogenesis.[43] In human burn wounds[44] and 1.14 and 1.5 mm deep FRDP dermatome wounds,[17] decorin has been reported as being suppressed early in the healing stage, and increasing to near normal levels in late stage healing. All injury methods in this work resulted in low expression levels at day 10, with the lowest being burn wounds at day 10, and increasing until day 150. Conversely, Scott et al. suggested that versican, whose presence is significantly increased in human HTS[45] and 1.14–1.5 mm deep FRDP dermatome wounds, interferes with proper collagen fibril formation.[45] Versican expression was increased in all wounds, with dermatome wounds peaking at day 28 and burn wounds peaking at day 90. IGF-1 has also been implicated in the development of HTS.[46] IGF-1 has been shown to increase fibroblast collagen production in vitro[46] and to increase collagen I mRNA and reduce collagenase mRNA expression in HTS derived fibroblasts.[25] Previously, in FRDP dermatome wounds, IGF-1 was heightened at day 10 decreasing through day 150.[17] IGF-1 expression in dermatome wounds in this work showed a similar trend, peaking at day 10; however, IGF-1 expression remained elevated in burn wounds from day 10 to day 28. In the current study, collagen type I and type III expression in burn scars remained significantly up-regulated at day 150 whereas excised wounds had returned to baseline. In human HTS, type I and type III procollagen were significantly upregulated compared to normal skin.[42] MMP2, which has been previously been shown to be present at higher levels in human hypertrophic and keloid scars compared to normal skin,[47] was expressed at greater levels in burn wounds than excisional wounds in this study. Collectively, these results suggest a greater delay in the healing process of burn scars than seen in scars resulting from dermatome injury, despite the apparent initial depth of injury being similar. As one might expect, the mechanism of injury impacts the healing.

Overall, within this study the burn model resulted in scars that were more raised, more contracted, more erythematic, possessed myofibroblasts, had blunted rete ridge formation and contained some similarities in collagen organization with human HTS when compared with the excisional model (Table 1). It is important to note that prior studies with the excisional model have shown improved similarities with human HTS than observed currently. This could be accounted for by small, but critical, differences in depth of injury created, postinjury care, microbiome differences, or genetic differences. It is possible that the genetic background of red Duroc pigs varies slightly among vendors and may be responsible for difference in observed outcomes. Gallant-Behm et al.[48] reported strong genetic involvement in the healing and fibrosis in Yorshire and Duroc cross breeds thus even a small genetic variation between herds may result in observable differences in scarring despite utilizing the same injury.

As with any animal model for human disease, the limitations of the current scar model must be considered. Although porcine skin possesses great similarity to human skin, several differences remain including skin thickness. Reported values of skin thickness (epidermis + dermis) from the back of middle aged humans ranged from 3 to 4.2 mm whereas the thickness of skin on the dorsum of the red Duroc pigs used for this study ranged from 5.4 to 7.2 mm. Thus a significant portion of injured dermis remains following the dermatome excisions and to a lesser extent following burn injury. As such, both the uninjured and remodeled tissues contribute to the biological and mechanical properties of the scars formed using the excision or burn model. These differences in skin thickness, specifically dermal thickness, may result in different fractions of papillary and reticular dermis remaining following injury and thus differences in scarring. In addition, the current porcine model utilizes juvenile pigs to allow for ease of housing and handling during the long study period. As a result these pigs grow significantly, more than tripling their body mass over the study period and this increase in body mass and total skin area can convolute measurements

Table 1. Comparison of the physical properties and tissue anatomy in scars resulting from excisional injuries and burn injuries in female red Duroc models vs. human hypertrophic scar.

Property	Porcine* shallow dermatome injury model	Porcine* deep dermatome injury model	Porcine* burn injury model	Human hypertrophic scar
Physical properties:				
Height	Not raised above normal skin	Not raised above normal skin	Raised 1–3 mm above normal tissue; gradual edge	Raised up to 1 cm above normal tissue; abrupt edge
Contraction	Not contracted	Moderate contraction	Excessive contraction	Excessive contraction
Pigmentation	Hyperpigmented	Hyperpigmented	Mixed hyper/hypopigmented	Hyperpigmented but occasionally mixed hyper/hypopigmented
Erythema	Minimal	Minimal	Moderate	Moderate to significant
Tissue anatomy:				
Presence of hair	Present	Absent	Absent	Largely absent
Rete pegs	Present	Present	Flattened with lower density	Largely absent, when present flattened
Collagen fiber organization (bundling and organization)	Disorganized with orthogonal ply pattern	Disorganized with orthogonal ply pattern	Disorganized with dense curvilinear bundles	Disorganized with whorls, frequent nodules
Presence of myofibroblasts	No	No	Yes	Yes

*"Porcine" refers to FRDP model, as described in the text.

of scar contraction. Despite these potential limitations, this porcine burn model more closely resembles excessive human scarring than excision models (under the described conditions), and serves as a model to allow future study of the efficacy of anti-scar therapy and a testbed for the development of new therapies. The findings also highlight the necessity, and challenges, of controlling for a multitude of factors that are part of the complex interplay of wound healing and scar formation.

CONCLUSIONS

The burn scar model presented in this study resulted in hairless, hyper/hypopigmented scars that were thicker, more erythematic, weaker, less elastic, and less pliable than scars formed using a dermatome model. These scars demonstrated more similarities to human HTS compared to dermatome wounds. As a result, this burn model may provide an improved platform for studying the pathophysiology of burn-related hypertrophic scarring and for investigating current anti-scar therapies and development of new strategies with greater clinical benefit.

ACKNOWLEDGMENTS

Source of Funding: This project was supported by the Shriners Hospital Research Foundations Grants #85100 and #85400 (HMP) and was partially supported by NIH grant GM077185, GM069589, NR013898, NR015676 and DOD W81XWH-11–2-0142 (CKS).

Conflicts of Interest: The authors report no conflicts of interest.

REFERENCES

1. Atiyeh BS, El Khatib AM, Dibo SA. Pressure garment therapy (PGT) of burn scars: evidence-based efficacy. *Ann Burns Fire Disasters* 2013; 26: 205–12.
2. Ripper S, Renneberg B, Landmann C, Weigel G, Germann G. Adherence to pressure garment therapy in adult burn patients. *Burns* 2009; 35: 657–64.
3. Bock O, Schmid-Ott G, Malewski P, Mrowietz U. Quality of life of patients with keloid and hypertrophic scarring. *Arch Dermatol Res* 2006; 297: 433–8.
4. Juckett G, Hartman-Adams H. Management of keloids and hypertrophic scars. *Am Fam Physician* 2009; 80: 253–60.
5. Leventhal D, Furr M, Reiter D. Treatment of keloids and hypertrophic scars: a meta-analysis and review of the literature. *Arch Facial Plast Surg* 2006; 8: 362–8.
6. Rabello FB, Souza CD, Farina JA. Update on hypertrophic scar treatment. *Clinics* 2014; 69: 565–73.
7. Costa AM, Peyrol S, Porto LC, Comparin JP, Foyatier JL, Desmouliere A. Mechanical forces induce scar remodeling. Study in non-pressure-treated versus pressure-treated hypertrophic scars. *Am J Pathol* 1999; 155: 1671–9.
8. Kim JY, Willard JJ, Supp DM, Roy S, Gordillo GM, Sen CK, et al. Burn scar biomechanics after pressure garment therapy. *Plast Reconstr Surg* 2015; 136: 572–81.
9. Waibel J, Beer K, Narurkar V, Alster T. Preliminary observations on fractional ablative resurfacing devices: clinical impressions. *J Drugs Dermatol* 2009; 8: 481–5.
10. Alster TS. Improvement of erythematous and hypertrophic scars by the 585-Nm flashlamp-pumped pulsed dye-laser. *Ann Plast Surg* 1994; 32: 186–90.
11. Zhu KQ, Engrav LH, Gibran NS, Cole JK, Matsumura H, Piepkorn M, et al. The female, red Duroc pig as an animal model of hypertrophic scarring and the potential role of the cones of skin. *Burns* 2003; 29: 649–64.
12. Gauglitz GG, Korting HC, Pavicic T, Ruzicka T, Jeschke MG. Hypertrophic scarring and keloids: pathomechanisms and current and emerging treatment strategies. *Mol Med* 2011; 17: 113–25.
13. Seo BF, Lee JY, Jung SN. Models of abnormal scarring. *Biomed Res Int* 2013; 2013: 423147.
14. Davidson JM, Yu F, Opalenik SR. Splinting strategies to overcome confounding wound contraction in experimental animal models. *Adv Wound Care* 2013; 2: 142–8.
15. Silverstein P, Goodwin MN, Raulston GL, Pruitt BA. Hypertrophic scar in the experimental animal. In Longacre JJ (ed.) *The ultrastructure of collagen: its relation to the healing of wounds and to the management of hypertrophic scar*. Springfield, IL: Thomas, 1976: 213–36.
16. Gallant-Behm CL, Hart DA. Genetic analysis of skin wound healing and scarring in a porcine model. *Wound Rep Regen* 2006; 14: 46–54.
17. Zhu KQ, Engrav LH, Tamura RN, Cole JA, Muangman P, Carrougher GJ, et al. Further similarities between cutaneous scarring in the female, red Duroc pig and human hypertrophic scarring. *Burns* 2004; 30: 518–30.
18. Zhu KQ, Carrougher GJ, Gibran NS, Isik FF, Engrav LH. Review of the female Duroc/Yorkshire pig model of human fibroproliferative scarring. *Wound Repair Regen* 2007; 15: S32–SS9.
19. Gallant CL, Olson ME, Hart DA. Molecular, histologic, and gross phenotype of skin wound healing in red Duroc pigs reveals an abnormal healing phenotype of hypercontracted, hyperpigmented scarring. *Wound Repair Regen* 2004; 12: 305–19.
20. Vartak A. Pathophysiology of burn shock. In: Srarabashi S, Tiwari VK, Goel A, editors. *Principles and practice of burn care*. New Delhi, India: Jaypee Publishers, 2010: 37–41.
21. Kim JY, Dunham DM, Supp DM, Sen CK, Powell HM. Novel burn device for rapid, reproducible burn wound generation. *Burns* 2016; 42: 384–91.
22. Livak KJ, Schmittgen TD. Analysis of relative gene expression data using real-time quantitative PCR and the 2(T)(-Delta Delta C) method. *Methods* 2001; 25: 402–8.
23. Deitch EA, Wheelahan TM, Rose MP, Clothier J, Cotter J. Hypertrophic burn scars: analysis of variables. *J Trauma* 1983; 23: 895–8.
24. Machesney M, Tidman N, Waseem A, Kirby L, Leigh I. Activated keratinocytes in the epidermis of hypertrophic scars. *Am J Pathol* 1998; 152: 1133–41.
25. Ghahary A, Shen YJ, Nedelec B, Wang R, Scott PG, Tredget EE. Collagenase production is lower in post-burn hypertrophic scar fibroblasts than in normal fibroblasts and is reduced by insulin-like growth factor-1. *J Invest Dermatol* 1996; 106: 476–81.
26. Zhu KQ, Engrav LH, Armendariz R, Muangman P, Klein MB, Carrougher GJ, et al. Changes in VEGF and nitric oxide after deep dermal injury in the female, red Duroc pig - further similarities between female, Duroc scar and human hypertrophic scar. *Burns* 2005; 31: 5–10.

27. Argyris T. Kinetics of epidermal production during epidermal regeneration following abrasion in mice. *Am J Pathol* 1976; 83: 329–40.
28. Macri LK, Singer AJ, Taira BR, McClain SA, Rosenberg L, Clark RA. Immediate burn excision fails to reduce injury progression. *J Burn Care Res* 2013; 34: e153–60.
29. Engrav LH, Garner WL, Tredget EE. Hypertrophic scar, wound contraction and hyper-hypopigmentation. *J Burn Car Res* 2007; 28: 593–7.
30. Macri LK, Singer AJ, McClain SA, Crawford L, Prasad A, Kohn J, Clark RA. Immediate tangential excision accelerates wound closure but does not reduce scarring of mid-dermal porcine burns. *Ann Burns Fire Disasters* 2016; 29: 54–61.
31. Cubison TC, Pape SA, Parkhouse N. Evidence for the link between healing time and the development of hypertrophic scars (HTS) in paediatric burns due to scald injury. *Burns* 2006; 32: 992–9.
32. Dunn MG, Silver FH, Swann DA. Mechanical analysis of hypertrophic scar tissue: structural basis for apparent increased rigidity. *J Invest Dermatol* 1985; 84: 9–13.
33. Moshref SS, Mufti ST. Keloid and hypertrophic scars: comparative histopathological and immunohistochemical study. *JKAU: Med Sci* 2010; 17: 3–22.
34. Bellemare J, Roberge CJ, Bergeron D, Lopez-Valle CA, Roy M, Moulin VJ. Epidermis promotes dermal fibrosis: role in the pathogenesis of hypertrophic scars. *J Pathol* 2005; 206: 1–8.
35. Hakvoort TE, Altun V, Ramrattan RS, van der Kwast TH, Benner R, van Zuijlen PP, et al. Epidermal participation in post-burn hypertrophic scar development. *Virchows Archiv* 1999; 434: 221–6.
36. Ghahary A, Marcoux Y, Karimi-Busheri F, Li Y, Tredget EE, Kilani RT, et al. Differentiated keratinocyte-releasable stratifin (14–3-3 sigma) stimulates MMP-1 expression in dermal fibroblasts. *J Invest Dermatol* 2005; 124: 170–7.
37. Linares HA, Larson DL. Early differential diagnosis between hypertrophic and nonhypertrophic healing. *J Invest Dermatol* 1974; 62: 514–6.
38. Harunari N, Zhu KQ, Armendariz RT, Deubner H, Muangman P, Carrougher GJ, et al. Histology of the thick scar on the female, red Duroc pig: final similarities to human hypertrophic scar. *Burns* 2006; 32: 669–77.
39. Santucci M, Borgognoni L, Reali UM, Gabbiani G. Keloids and hypertrophic scars of Caucasians show distinctive morphologic and immunophenotypic profiles. *Virchows Arch* 2001; 438: 457–63.
40. Kamath NV, Ormsby A, Bergfeld WF, House NS. A light microscopic and immunohistochemical evaluation of scars. *J Cutan Pathol* 2002; 29: 27–32.
41. Tredget EE, Shankowsky HA, Pannu R, Nedelec B, Iwashina T, Ghahary A, et al. Transforming growth factor-beta in thermally injured patients with hypertrophic scars: effects of interferon alpha-2b. *Plast Reconstr Surg* 1998; 102: 1317–28, discussion 29–30.
42. Ghahary A, Shen YJ, Scott PG, Gong Y, Tredget EE. Enhanced expression of mRNA for transforming growth factor-beta, type I and type III procollagen in human post-burn hypertrophic scar tissues. *J Lab Clin Med* 1993; 122: 465–73.
43. Danielson KG, Baribault H, Holmes DF, Graham H, Kadler KE, Iozzo RV. Targeted disruption of decorin leads to abnormal collagen fibril morphology and skin fragility. *J Cell Biol* 1997; 136: 729–43.
44. Sayani K, Dodd CM, Nedelec B, Shen YJ, Ghahary A, Tredget EE, et al. Delayed appearance of decorin in healing burn scars. *Histopathology* 2000; 36: 262–72.
45. Scott PG, Dodd CM, Tredget EE, Ghahary A, Rahemtulla F. Immunohistochemical localization of the proteoglycans decorin, biglycan and Versican and transforming growth-factor-beta in human postburn hypertrophic and mature scars. *Histopathology* 1995; 26: 423–31.
46. Ghahary A, Shen YJ, Nedelec B, Scott PG, Tredget EE. Enhanced expression of mRNA for insulin-like growth factor-1 in post-burn hypertrophic scar tissue and its fibrogenic role by dermal fibroblasts. *Mol Cellular Biochem* 1995; 148: 25–32.
47. Tanriverdi-Akhisaroglu S, Menderes A, Oktay G. Matrix metalloproteinase-2 and −9 activities in human keloids, hypertrophic and atrophic scars: a pilot study. *Cell Biochem Funct* 2009; 27: 81–7.
48. Gallant-Behm CL, Reno C, Tsao H, Hart DA. Genetic involvement in skin wound healing and scarring in domestic pigs: assessment of molecular expression patterns in (Yorkshire x Red Duroc) x Yorkshire backcross animals. *J Invest Dermatol* 2007; 127: 233–44.